Available online at www.sciencedirect.com
SCIENCE DIRECT®

Journal of Colloid and Interface Science 278 (2004) 270–275

Journal of Colloid and Interface Science
www.elsevier.com/locate/jcis

Adsorption of arsenate and arsenite on titanium dioxide suspensions

Paritam K. Dutta [a], Ajay K. Ray [a], Virender K. Sharma [b,*], Frank J. Millero [c]

[a] Department of Chemical and Biomolecular Engineering, National University of Singapore, 10 Kent Ridge Crescent, Singapore 119260
[b] Chemistry Department, Florida Institute of Technology, 150 West University Boulevard, Melbourne, FL 32901, USA
[c] Rosenstiel School of Marine and Atmospheric Chemistry, University of Miami, 4600 Rickenbacker Causeway, Miami, FL 33149, USA

Received 7 October 2003; accepted 1 June 2004

Abstract

Adsorption of arsenate (As(V)) and arsenite (As(III)) to two commercially available titanium dioxide (TiO_2) suspensions, Hombikat UV100 and Degussa P25, was investigated as a function of pH and initial concentration of adsorbate ions. The BET surface area and zeta potential values of TiO_2 were also measured to understand the difference in adsorption behavior of two suspensions. Both As(V) and As(III) adsorb more onto Hombikat UV100 particles than Degussa P25 particles. Adsorption of As(V) onto TiO_2 suspensions was more than As(III) at pH 4 while the adsorption capacity of As(III) was more at pH 9. The electrostatic factors between surface charge of TiO_2 particles and arsenic species were used to explain adsorption behavior of As(V) and As(III) at different pH. The Langmuir and Freundlich isotherm equations were used to interpret the nature of adsorption of arsenic onto TiO_2 suspensions. The usefulness of adsorption data in removing arsenic in water is briefly discussed.

Keywords: Arsenate; Arsenite; Titanium dioxide; Adsorption; Point of zero charge; Isotherms

---

1. Introduction

Arsenic [arsenite (As(III)) and arsenate (As(V))] contamination in groundwater has become a major concern in many countries including Bangladesh, Vietnam, and the western United States [1]. The main source of arsenic is geological, but human activities such as mining and pesticides can also cause arsenic pollution. The toxicity of arsenic to human health ranges from skin lesions to cancer of brain, liver, kidney, and stomach [2]. Recently, the European Union and the United States governments have therefore lowered the maximum contaminant level for total arsenic to 10 μg/L in drinking water.

The distribution between As(III) and As(V) in water depends on redox potential and pH [3,4]. Under groundwater conditions, As(III) is the predominate form of arsenic, which is more toxic and mobile than As(V) [1]. As(III) has low affinity with mineral surfaces while As(V) adsorbs easily to solid surfaces. The most common method of arsenic removal is coagulation with iron salts and alum, followed by microfiltration [5–7]. The oxidation of As(III) to As(V) is therefore highly desirable to achieve As(V) adsorption onto metal oxyhydroxides [8–11].

The oxidation of As(III) to As(V) can be accomplished by photocatalytic reactions using titanium dioxide (TiO_2) as a catalyst [12,13]. The adsorption of arsenic ions onto TiO_2 plays an important role during the photocatalytic reaction. Hombikat UV100 and Degussa P25 are two commercially available TiO_2 samples. The study on adsorption of arsenic onto Degussa P25 TiO_2 has been performed, but similar studies with Hombikat UV100 TiO_2 have not been carried out. In this paper, studies of arsenic adsorption onto Hombikat UV100 TiO_2 were carried out in the pH range from 3 to 9. Studies with Degussa P25 TiO_2 were also performed under identical experimental conditions for comparison. The objectives of the present study were twofold: (1) to investigate the pH dependence of As(III) and As(V) adsorption onto two TiO_2 suspensions at varying initial arsenic concentrations; and (2) to describe the data using adsorption isotherms.

---

[*] Corresponding author.
E-mail address: vsharma@fit.edu (V.K. Sharma).

0021-9797/$ – see front matter © 2004 Elsevier Inc. All rights reserved.
doi:10.1016/j.jcis.2004.06.015

Table 1
Physicochemical properties of titanium dioxide used in experiments

Property	Hombikat UV100	Degussa P25
Composition	99% anatase	≈80% anatase, ≈20% rutile
Density (g/cm^3)	3.9	3.8
BET surface area ($m^2\,g^{-1}$)[a]	334	≈55
Average primary particle (nm)[a]	<10	≈30
pH in aqueous solution	≈6	3–4
Porosity	Porous (mesoporous, ≈5.6 nm in diameter)	Non-porous

[a] Taken from Ref. [15].

2. Materials and methods

Analytical grade chemicals were used without further purification. Solutions were prepared in ultra pure water (resistivity 18.2 MΩ) obtained with a Milli-Q water purification system. Sodium arsenite, $NaAsO_2$, was used as a source of As(III) and was obtained from Fluka chemical. The source of As(V) was the sodium salt of arsenic acid, hepta hydrate, $Na_2HAsO_4{\cdot}7H_2O$ (Aldrich Chemical). Stock solutions containing 0.0015 M As(III) and As(V) were prepared and stored in a dark place to carry out the experiments. Degussa (Germany) and Sachtleben Chemie GmbH (Germany) provided the two titanium dioxide samples, Degussa P25 and Hombikat UV100, respectively.

The zeta potential, ξ, measurements of TiO_2 used aqueous suspensions prepared by adding 0.05 g to 1 L of 0.001 M $NaNO_3$. The pH was adjusted to the desired value by adding either HNO_3 or NaOH. These suspensions were shaken for 24 h in the dark, the ξ-potential was measured, and the final pH of the suspensions was recorded. The Brookhaven Zeta-Plus system was used to determine the zeta potentials.

Adsorption studies of As(III) and As(V) were carried out by adding the required amount of TiO_2 suspensions into either As(III) or As(V) solutions at different concentrations. After adjusting the pH of solutions to the desired values, solutions were sealed and stirred by magnetic stirrer at room temperature (295 ± 3 K). An Orion model 720A pH meter was used to measure the pH of the solution. A combination electrode was calibrated using commercial pH 4.0, 7.0, and 10.0 buffers. The suspensions were mixed continuously for about 2 h for Degussa P25 and 3 h for Hombikat UV100 to establish adsorption equilibrium. At the end of the equilibrium period, 10 ml of the mixture was filtered through 0.45 µm filter and the supernatant was analyzed for As(V) and total arsenic.

Inductively coupled plasma–optical emission spectroscopy (ICP–OES) (Perkin–Elmer Optima 3000DV) was used to measure total arsenic concentration (>7.5 µM) in the solution. The total arsenic concentrations lower than <1.5 µM were analyzed by inductively coupled plasma–mass spectroscopy (ICP–MS) (ELAN 6100, Perkin–Elmer) and whenever necessary the solution was diluted by ELGA 18.2 MΩ ultrapure water before analyzing to make sure the arsenic concentrations did not exceed 1.5 µM. As(V) was measured spectrophotometrically using the molybdenum blue method [14]. Concentrations of As(III) were determined by the difference between As(total) and As(V). The accuracy and precision of measurements were within ±5%.

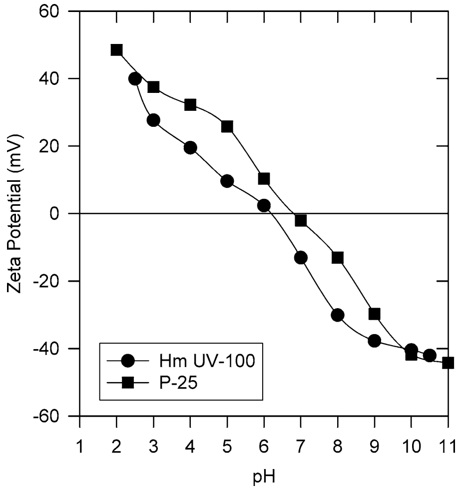

Fig. 1. Zeta potential of TiO_2 suspensions in 0.001 M $NaNO_3$ at different pH.

3. Results and discussion

3.1. Physicochemical characteristics of TiO_2 suspensions

The physicochemical data of two TiO_2 samples, Hombikat UV100 and Degussa P25, used in the study are given in Table 1. The characteristic differences between the two suspensions are their composition, BET surface area, and porosity. Hombikat UV 100 is composed of anatase while Degussa P25 is a combination of anatase and rutile surfaces of titanium dioxide [15]. The particle size of Hombikat UV100 is smaller than that of Degussa P25 (Table 1). This gives a much higher surface area of Hombikat UV100 than of Degussa P25.

The zeta potential, ξ, values were measured in 0.001 M $NaNO_3$ solutions in order to observe the surface charges of the TiO_2 suspensions. The values of zeta potential of TiO_2 suspensions as a function of pH are shown in Fig. 1. The points of zero charges (PZC) for Hombikat UV100 and Degussa P25 were obtained as 6.2 and 6.9, respectively. The PZC of Degussa P25 in our study is in reasonable agreement with the literature value of 6.8 ± 0.2 [16]. At pH < pH_{pzc},

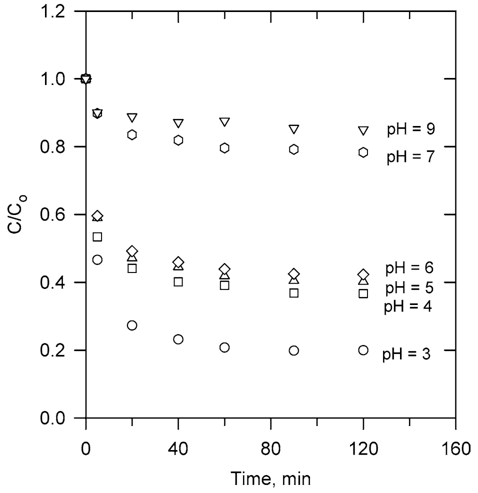

Fig. 2. Adsorption of As(V) on Hombikat UV100 TiO_2 suspension as a function of pH. $C_0 = 133$ µmol/L.

TiO_2 surface is positively charged (Eq. (1)) whereas at $pH > pH_{pzc}$ TiO_2 surface is negatively charged (Eq. (2)).

$$\mathrm{Ti^{IV}\text{–}OH + H^+ \rightarrow Ti^{IV}\text{–}OH_2^+}, \quad \mathrm{pH < pH_{pzc}}, \tag{1}$$

$$\mathrm{Ti^{IV}\text{–}OH + OH^- \rightarrow Ti^{IV}\text{–}O^- + H_2O}, \quad \mathrm{pH < pH_{pzc}}. \tag{2}$$

3.2. As(V) and As(III) adsorption equilibrium

As(V) and As(III) adsorption equilibria at various pH were established in approximately 2 and 1 h for Hombikat UV100 and Degussa P25, respectively. Hombikat UV100 TiO_2 is composed of mesoporous particles (Table 1) in which adsorption is possibly occurring through pore diffusion steps and takes a longer time to reach equilibrium. In comparison, Degussa P25 is made of nonporous TiO_2 particles where only intermolecular diffusion adsorption processes occur. This adsorption phenomenon would thus require less time to reach equilibrium.

The kinetics of As(V) adsorption onto Hombikat UV100 TiO_2 suspensions at different pH are shown in Fig. 2. The kinetics and amounts of As(V) adsorption onto TiO_2 suspensions were pH dependent; higher rates and amounts adsorbed occur at low pH. Similar pH dependence on the uptake of As(V) onto other oxide surfaces was found [8–12,17,18]. The As(V) adsorption kinetic data were found to be best described by the power function kinetic model [19], which can be described by the equation

$$\mathrm{As(V)}_t = kt^{\nu}, \tag{3}$$

where $\mathrm{As(V)}_t$ is amount of As(V) adsorbed at time t, and k and ν are rate constant and order, respectively, for adsorption process. A log–log plot of Eq. (3) is shown in Fig. 3. The values of ν and k obtained from the plot are given in Table 2. A fractional order, 0.12 ± 0.02 adsorption process was found, which was independent of pH. Fractional orders are not uncommon in heterogeneous systems [20]. The rate constants decrease with increase in pH (Fig. 4A). In the system, anatase surface of Hombikat UV100 is considered monoprotic [21] (Eq. (4)) and As(V) is triprotic acid [18] (Eqs. (5)–(7)).

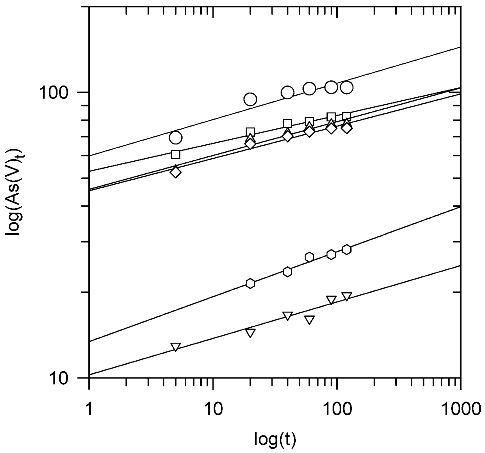

Fig. 3. A plot of As(V) adsorption data using a power function kinetic model (Eq. (3)). pH 3 (○); pH 4 (□); pH 5 (△); pH 6 (◇); pH 7 (○); pH 9 (▽).

Table 2
Power function kinetic model parameters for adsorption of As(V) on Hombikat UV100 TiO_2 catalyst at different pH

pH	k (µmol $(\mathrm{g\text{-}TiO_2})^{-1}$ $\mathrm{min}^{0.12}$)	ν	r^2
3	59.9 ± 0.89	0.13 ± 0.02	0.88
4	52.9 ± 0.32	0.10 ± 0.01	0.96
5	45.8 ± 0.47	0.12 ± 0.02	0.94
6	45.2 ± 0.40	0.11 ± 0.01	0.95
7	13.4 ± 0.13	0.16 ± 0.02	0.96
9	10.2 ± 0.22	0.13 ± 0.02	0.92

$$\mathrm{Ti^{IV}\text{–}OH_2^+ \rightleftarrows H^+ + Ti^{IV}\text{–}OH}, \quad \mathrm{p}K_s = 4.58\ [21], \tag{4}$$

$$\mathrm{AsO(OH)_3 \rightleftarrows H^+ + AsO_2(OH)_2^-}, \quad \mathrm{p}K_{a1} = 2.3, \tag{5}$$

$$\mathrm{AsO_2(OH)_2^- \rightleftarrows H^+ + AsO_3(OH)^{2-}}, \quad \mathrm{p}K_{a2} = 6.8, \tag{6}$$

$$\mathrm{AsO_3(OH)^{2-} \rightleftarrows H^+ + AsO_4^{3-}}, \quad \mathrm{p}K_{a3} = 11.6. \tag{7}$$

The rate dependence can then be analyzed by considering attractions between the positive surfaces sites of TiO_2 with four species of As(V), $\mathrm{AsO(OH)_3}$, $\mathrm{AsO_2(OH)_2^-}$, $\mathrm{AsO_3(OH)^{2-}}$, and $\mathrm{AsO_4^{3-}}$ (Eqs. (8)–(11)).

$$\mathrm{Ti^{IV}\text{–}OH_2^+ + AsO(OH)_3 \xrightarrow{k_1} Ti^{IV}\text{–}OH_2^+ \bullet\bullet AsO(OH)_3}, \tag{8}$$

$$\mathrm{Ti^{IV}\text{–}OH_2^+ + AsO_2(OH)_2^-} \\ \mathrm{\xrightarrow{k_2} Ti^{IV}\text{–}OH_2^+ \bullet\bullet AsO_2(OH)_2^-}, \tag{9}$$

$$\mathrm{Ti^{IV}\text{–}OH_2^+ + AsO_3(OH)^{2-}} \\ \mathrm{\xrightarrow{k_3} Ti^{IV}\text{–}OH_2^+ \bullet\bullet AsO_3(OH)^{2-}}, \tag{10}$$

$$\mathrm{Ti^{IV}\text{–}OH_2^+ + AsO_4^{3-} \xrightarrow{k_4} Ti^{IV}\text{–}OH_2^+ \bullet\bullet AsO_4^{3-}}. \tag{11}$$

The rate constant, k, as a function of pH can be given by the equation

$$k = \big\{\big(k_1[\mathrm{H}^+]^3 + k_2K_{a1}[\mathrm{H}^+]^2 + k_3K_{a1}K_{a2}[\mathrm{H}^+] \\ + k_4K_{a1}K_{a2}K_{a3}\big)\big([\mathrm{H}^+]\big/\big([\mathrm{H}^+] + K_s\big)\big)\big\}/Z, \tag{12}$$

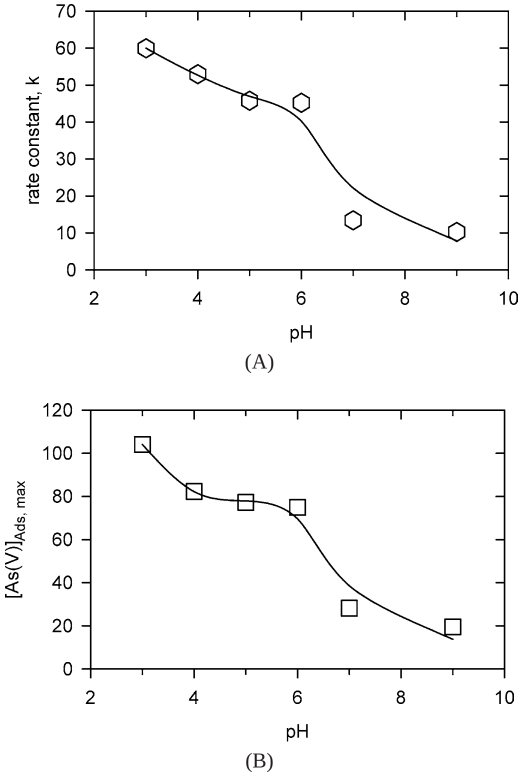

(A)

(B)

Fig. 4. *k* (A) and maximum As(V) (B) as a function of pH.

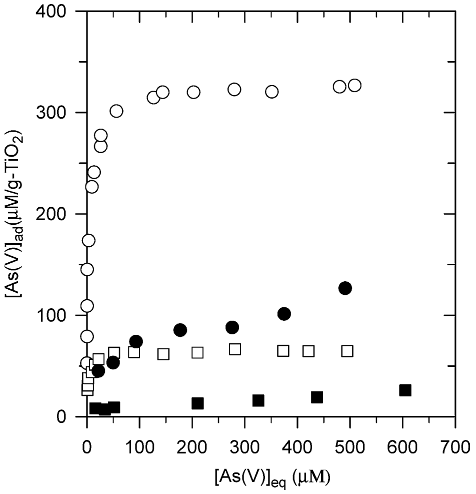

Fig. 5. Adsorption of As(V) on Hombikat UV100 (circle) and Degussa P25 TiO_2 (square) suspensions at two different pH. pH 4 (open symbols); pH 9 (filled symbols).

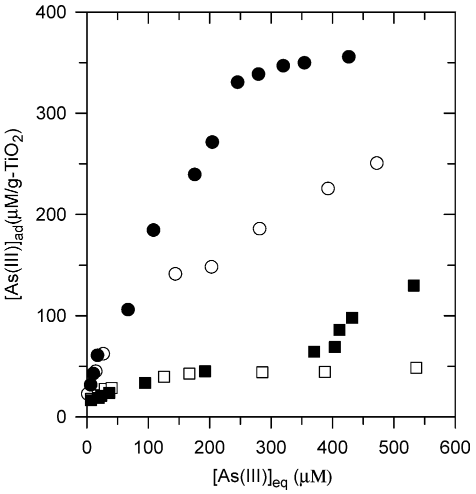

Fig. 6. Adsorption of As(III) on Hombikat UV100 (circle) and Degussa P25 TiO_2 (square) suspensions at two different pH. pH 4 (open symbols); pH 9 (filled symbols).

where $Z = [H^+]^3 + K_{a1}[H^+]^2 + K_{a1}K_{a2}[H^+] + K_{a1}K_{a2}K_{a3}$. The non-linear regression fit of the data gave $k_1 = 9.2 \pm 6.0 \times 10^1$, $k_2 = 5.4 \pm 0.1 \times 10^1$, $k_3 = 7.5 \pm 0.1 \times 10^3$, and $k^4 = 8.0 \times 10^7$ µmol $(\text{g-TiO}_2)^{-1}\,\text{min}^{0.12}$. These values give a reasonable fit to the estimated rate constants (a solid line in Fig. 4A). As expected the interaction of AsO_4^{3-} with $Ti^{IV}–OH_2^+$ surface is dominant at low pH. The maximum adsorption amount of As(V) as a function of pH is shown in Fig. 4B. At pH < pH_{pzc}, the TiO_2 surface has a net positive charge (Eq. (4)) that attracts the As(V) anions to give higher amounts of adsorption at low pH.

The As(V) equilibrium experiments of adsorption onto TiO_2 suspension at pH 4 and 9 were conducted to develop isotherms and the results are shown in Fig. 5. At both pH values, the adsorption capacity of As(V) onto Hombikat UV100 suspension was higher than onto Degussa P25 TiO_2. This is due to the higher surface area for Hombikat UV100 TiO_2 particles compared to Degussa P25. The difference in porosity may also play a role in the different adsorption capacities of the two TiO_2 suspensions.

The experiment results for the As(III) adsorption onto TiO_2 are presented in Fig. 6. Similar to As(V), As(III) adsorption capacities onto Hombikat UV100 TiO_2 particles were higher than onto Degussa P25 suspensions in both acidic and alkaline medium. However, the adsorption of As(III) onto TiO_2 particles increases with increases in pH, which is opposite to the adsorption behavior found for As(V). As(III) behaves like a weak acid and goes through equilibrium represented by the equations [22]

$$As(OH)_3 \rightleftarrows H^+ + AsO(OH)_2^-, \quad pK_1 = 9.23, \tag{13}$$

$$AsO(OH)_2^- \rightleftarrows H^+ + AsO_2(OH)^{2-}, \quad pK_2 = 12.10, \tag{14}$$

$$AsO_2(OH)^{2-} \rightleftarrows H^+ + AsO_3^{3-}, \quad pK_3 = 13.41. \tag{15}$$

At pH 4, neutral species ($As(OH)_3$) predominate and approximately equimolar mixtures of $As(OH)_3$ and $AsO(OH)_2^-$ are present at pH 9 (Eqs. (13)–(15)). Increase of As(III) adsorption in alkaline solution suggests that the simple electrostatic factors are not controlling the adsorption of As(III) onto TiO_2 particles. In alkaline solution, the release of proton from $As(OH)_3$ (Eq. (13)) may remove the hydroxyl ion from the coordinating layer of the TiO_2 surface (Eq. (4)). This process creates sites with positive charge at the surface of TiO_2 to adsorb negative As(III) anions at alkaline pH.

Table 3
Isotherm parameters for adsorption of As(V) and As(III) on Degussa P25 and Hombikat UV100 TiO_2 catalyst at different pH

	pH	Langmuir isotherm equation			Freundlich isotherm equation		
		Q_{sat}	K_{ad} (10^{-6} M^{-1})	r^2	n	K_F	r^2
		Hombikat UV100					
As(V)	4	300 ± 79	1.2 ± 0.3	0.98	7.2 ± 0.8	152 ± 11	0.90
	9	121 ± 3	0.02 ± 0.01	0.85	3.1 ± 0.4	16 ± 3	0.94
As(III)	4	303 ± 65	0.007 ± 0.002	0.86	2.1 ± 0.1	13 ± 2	0.99
	9	575 ± 69	0.005 ± 0.001	0.98	1.8 ± 0.2	13 ± 0.4	0.99
		Degussa P25					
As(V)	4	62 ± 9	0.5 ± 0.1	0.93	8.9 ± 0.8	35 ± 2	0.86
	9	23 ± 1	0.012 ± 0.007	0.74	2.5 ± 0.4	1.8 ± 0.7	0.90
As(III)	4	46 ± 7	0.05 ± 0.01	0.94	4.6 ± 0.3	13 ± 1	0.96
	9	52 ± 32	0.05 ± 0.01	0.68	1.4 ± 0.3	14 ± 1	0.88

Similar patterns for adsorption of As(V) and As(III) onto iron and aluminum oxide surfaces as a function of pH have been found [8–11]. The adsorption of arsenic onto ferrihydrite showed changes in surface charge properties of the adsorbent during the process in the pH range of 4–10 [10]. The property of surface charge is related to whether there is net release of either H^+ or OH^- ion during the adsorption process. As(V) adsorption results in the release of OH^- ions at pH 4.6 and 9.2. In comparison, the adsorption of As(III) at acidic pH releases H^+ while OH^- is released at basic pH. There is an increase in the negative character of the surface adsorbing As(V) onto hydroxylated surfaces with increasing pH, hence greater adsorption of As(V) at low pH. As(III) treated surfaces did not show a change in the negative character of surfaces and therefore greater adsorption of As(III) at higher pH. A similar adsorption mechanism of As(V) and As(III) onto TiO_2 surfaces may occur causing larger amounts of As(V) at low pH and As(III) at high pH. Another possibility is the formation of complexes with surface structural titanium dioxide sites, which may vary with pH. Spectroscopic and model studies with iron oxide surfaces have shown that As(V) forms a combination of mono- and bi-dentate complexes and a single bidentate binuclear complex is obtained with As(III) [23–26]. The adsorption of arsenic on amorphous aluminum and iron oxides has suggested the pH dependence in the position of As–O stretching bonds for both As(III) and As(V) [18].

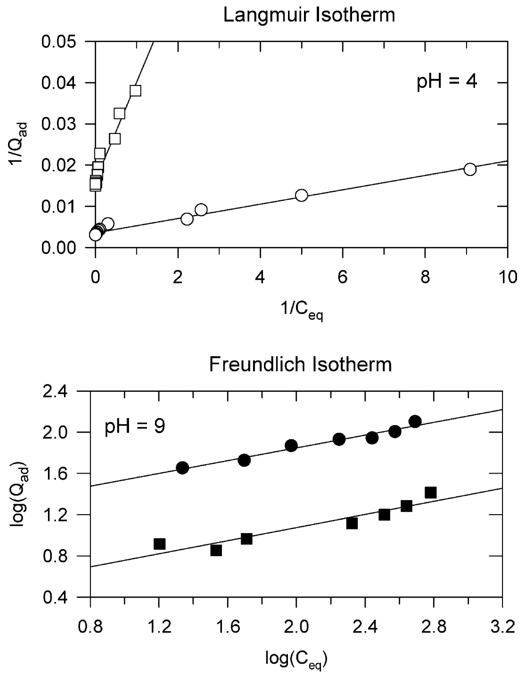

Fig. 7. Langmuir and Freundlich adsorption isotherms for adsorption of As(V) on Hombikat UV100 (circle) and Degussa P25 TiO_2 (square) suspensions at two different pH. pH 4 (open symbols); pH 9 (filled symbols).

3.3. Adsorption isotherms

The two most common models to describe adsorption process are the two-parameter isotherms of Langmuir and Freundlich. The Langmuir adsorption isotherm can be described by the equation

$$Q_{ad} = Q_{sat} \frac{K_{ad} C_{eq}}{1 + K_{ad} C_{eq}}, \tag{16}$$

where Q_{ad} is the specific adsorbed quantity of a model compound and C_{eq} is the pollutant concentration, both at equilibrium; Q_{sat} is the saturation (maximum) adsorption capacity and K_{ad} is the adsorption constant. Unique adsorption sites, monolayer adsorption, and no interaction between the adsorption sites are the underlying assumptions used in deriving the Langmuir isotherm.

On the other hand, the Freundlich adsorption isotherm equation can be expressed by the equation

$$Q_{ad} = K_F C_{eq}^{1/n}, \tag{17}$$

where K_F and n are two Freundlich isotherm parameters.

Adsorption data of As(V) obtained from experiments at pH 4 for both Hombikat UV100 and Degussa P25 TiO_2 surfaces fit well with the Langmuir equation, but the Freundlich equation gives a better adsorption of As(V) at pH 9 (Fig. 7). The parameters obtained using non-linear least squares treatment of data for both Langmuir and Freundlich isotherms for As(V) at pH 4 and 9 are given in Table 3. The value of $K_{ad} = 6.7 \pm 0.4 \times 10^5\ M^{-1}$ As(V) adsorption at pH 4 for Degussa P25 TiO_2 suspensions is in reasonable agreement with the literature value of $6 \times 10^5\ M^{-1}$ at pH 3 [13]. Experimental data of As(III) adsorption on TiO_2 at pH 4 and 9 gave a better fit using the Freundlich isotherm (Table 3). The isotherm parameters for As(III) at pH 4 and 9 on Hombikat UV100 as well as Degussa P25 are also given in Table 3.

The dependence of adsorption on two different isotherms may be explained by considering that the oxide surfaces have different kinds of surface sites with different affinities for adsorbate ions, As(V) and As(III) [27]. The density of strong binding sites may be much less than the weaker binding sites of the oxide surfaces. If adsorption occurs until all the strong binding sites are occupied, adsorption process follow Langmuir isotherm, as was found for As(V) at pH 4. The Freundlich isotherm fits for As(V) at pH 9 and As(III) at pH 4 and 9 indicate heterogeneity of the surface due to involvement of both strong and weaker binding sites for adsorption, thus resulting in a multisite adsorption processes for these adsorbate ions.

4. Conclusion

The results of Figs. 5 and 6 suggest that adsorption of As(V) is very much higher than As(III) adsorption at pH 4, especially at low equilibrium concentrations of As(V). Comparatively, adsorption of As(III) is much higher than that of As(V) at pH 9. In natural waters, arsenic is usually present at very low concentration; oxidation of As(III) to As(V) followed by subsequent adsorption of As(V) on TiO_2 surface at slightly acidic media would completely remove arsenic from the water. The photocatalysis process under ultraviolet and visible radiation can achieve oxidation of As(III) at low TiO_2 suspension. Additionally, TiO_2 surfaces adsorbs less As(V) at $pH > pH_{pzc}$ and strongly adsorb at $pH < pH_{pzc}$; the catalyst can be easily regenerated for further use by raising the pH.

The adsorption of As(V) and As(III) onto commercially available TiO_2 in aqueous solution is controlled by both the surface charge of TiO_2 and the form of arsenic species. The pH is therefore a strong factor in adsorption of both As(V) and As(III) by TiO_2. The adsorption capacity of As(V) is high in acidic solutions while that of As(III) is high in basic solutions. These results suggest that under basic conditions TiO_2 photocatalyst is more efficient for the oxidation of As(III) to As(V). The removal of As(V) from water by adsorption onto TiO_2 can then be maximized by adjusting the pH to acidic environment.

Acknowledgments

We acknowledge the financial support from the Academic Research Council (ARC), National University of Singapore (NUS) under research grant number R-279-000-128-112. F.J.M. acknowledges the support of the oceanic section of the National Science Foundation. The authors thank an anonymous reviewer for improving the manuscript.

References

[1] J.S. Wang, C.M. Wai, J. Chem. Educ. 81 (2004) 207.

[2] A.H. Smith, C. Hopenhayn, M.N. Bates, H.M. Goeden, I.H. Picciotto, H.M. Duggan, R. Wood, M.J. Kosnett, M.T. Smith, Environ. Health Perspect. 97 (1992) 259.

[3] W.R. Cullen, K.J. Reimer, Chem. Rev. 89 (1989) 713.

[4] P.H. Masscheleyn, R.D. Delaune, W.H. Patrick Jr., Environ. Sci. Technol. 25 (1991) 1414.

[5] M.J. DeMarco, A.K. SenGupta, J.E. Greenleaf, Wat. Res. 37 (2003) 164.

[6] N.P. Nikolaidis, G.M. Dobbs, J.A. Lackovic, Wat. Res. 37 (2003) 1417.

[7] J.G. Hering, P.-Y. Chen, J.A. Wilkie, M. Elimelech, S. Liang, J. Amer. Water Works Assoc. 88 (1996) 155.

[8] T.-F. Lin, J.-K. Wu, Wat. Res. 35 (2001) 2049.

[9] A. Jain, R.H. Loeppert, J. Environ. Qual. 29 (2000) 1422.

[10] K.P. Raven, A. Jain, R.H. Loeppert, Environ. Sci. Technol. 32 (1998) 344.

[11] A. Jain, K.P. Raven, R.H. Loeppert, Environ. Sci. Technol. 33 (1999) 1179.

[12] M. Bissen, M.-M. Vieillard-Baron, A.J. Schindelin, F.H. Frimmel, Chemosphere 44 (2001) 751.

[13] H. Lee, W. Choi, Environ. Sci. Technol. 36 (2002) 3872.

[14] E.B. Sandell, Colorimetric Determination of Trace of Metals, vol. 3, Chemical Analysis, New York, 1959.

[15] B. Sun, P.J. Smirniotis, Catalysis Today 88 (2003) 49.

[16] P. Fernandez-Ibanez, F.J.D.L. Nieves, S. Malato, J. Colloid Interface Sci. 227 (2000) 510.

[17] O.S. Thirunavukkarasu, T. Viraraghavan, K.S. Subramanian, Wate Air Soil. Pollut. 142 (2003) 95.

[18] S. Goldberg, C.T. Johnston, J. Colloid Interface Sci. 234 (2001) 204.

[19] D.L. Sparks, Soil Physical Chemistry, second ed., CRC Press, Boca Raton, FL, 1999.

[20] H. Yoneyama, Y. Yamashita, H. Tamura, Nature 282 (1979) 817.

[21] N. Spanos, I. Georgiadou, A. Lycourghiotis, J. Colloid Interface Sci. 172 (1995) 374.

[22] D.S. Brown, J.D. Allison, An Equilibrium Metal Speciation Model: Users Manual. Env. Res. Lab., Office of Res. and Dev. U.S. Environmental Protection Agency, Rept. No. EPA/600/3-87/012 (1987).

[23] W. Stumm, Chemistry of the Solid–Water Interface, Wiley, New York, 1992.

[24] T. Hiemstra, W.H. Van Riemsdijk, J. Colloid Interface Sci. 210 (1999) 182.

[25] T.H. Hsia, S.L. Lo, C.F. Lin, Colloids Surf. A 5 (1994) 1.

[26] B.A. Manning, S.E. Fendorf, S. Goldberg, Environ. Sci. Technol. 32 (1998) 2383.

[27] M.L. Pierce, C.B. Moore, Wat. Res. 16 (1982) 1247.